An efficient method for calculating system reliability of soil slope with general shape slip surfaces

Indexed by:
Web of Science Group

Juxiang Chen[a,*], Dayong Zhu[b], Yalin Zhu[a,c], Yixian Wang[a,c]

[a] College of Civil and Hydraulic Engineering, Hefei University of Technology, China
[b] School of Civil Engineering and Architecture, Ningbo Tech University, China
[c] Anhui Key Laboratory of Civil Engineering Structures and Materials, China

Highlights

- An efficient system reliability calculation method is proposed for soil slopes with general slip surfaces.

- The performance function uses the critical horizontal seismic acceleration coefficient expression to replace the traditional safety factor expression.

- This method can quickly identify the main representative slip surfaces and effectively calculate the reliability of the slope system with only a small amount of calculation.

Abstract

Reliability analysis of slope stability is essentially a system reliability problem. The traditional reliability calculation method of slope system based on limit equilibrium adopts the safety factor expression as the performance function. The safety factor is usually a nonlinear implicit function, which needs to be solved iteratively, so it is difficult to balance the calculation accuracy and efficiency. Moreover, it is generally assumed that the slip surface is circular, which is inconsistent with the actual situation. Based on the rigorous limit equilibrium method by modifying normal stress over slip surface, an explicit performance function expressed by critical horizontal acceleration coefficient K_c is established. A slope system reliability calculation method coupling Rosenblueth sampling point method, global critical sliding field (GCSF) method and sequential compounding method (SCM) is proposed. The accuracy and high efficiency of the proposed method are verified by two slope examples. It can be used as a powerful tool for rapid assessment of slope stability reliability.

Keywords

slope system reliability, global critical sliding field, general shape slip surface, critical horizontal acceleration factor, sequential compounding method

1. Introduction

Slope stability evaluation is one of the important topics in the field of geotechnical engineering. The reliability analysis of slope stability can quantitatively consider the uncertainty of soil parameters, which is considered as a useful supplement to the deterministic method [1]. Most slopes contain multiple soil layers, and the soil parameters have inherent variability. These factors may cause the slope to fail along multiple different slip surfaces. Sliding along any slip surface will lead to slope failure.

The slope is a series structure system with multiple failure modes. The reliability analysis of slope stability is essentially to calculate its system reliability.

Based on the deterministic method of slope stability, the traditional slope reliability analysis method establishes the performance function expressed by the safety factor, and then combines the reliability analysis method to calculate the reliability index and failure probability. The deterministic

(*) Corresponding author.
E-mail addresses: J. Chen (ORCID: 0000-0002-9662-8788) chenjx@hfut.edu.cn, D. Zhu: zhudymeng@163.com, Y. Zhu (ORCID: 0000-0001-5234-4276) zhuyalin@hfut.edu.cn, Y. Wang (ORCID: 0000-0002-2346-3097) wangyixian2012@hfut.edu.cn

methods of slope stability mainly include limit equilibrium method (LEM), limit analysis method (LAM) and finite element method (FEM). FEM can truly reflect the stress state in the soil and automatically locate the critical slip surface, which is especially suitable for slopes with complex soil layers. LAM constructs the static allowable stress field or the maneuvering allowable velocity field according to the upper or lower limit theorem, and uses the mathematical programming method to solve the safety factor. LEM needs to assume the position and shape of the slip surface, and the safety factor is solved by studying the static equilibrium of the forces and torques acting on the slip surface. Because of its clear concept and high computational efficiency, it is still the main method for evaluating slope stability in engineering field.

The commonly used reliability analysis methods mainly include Monte Carlo simulation (MCS), first-order reliability method (FORM) and response surface method (RSM). MCS method is recognized as the most direct and effective method among these methods. However, there are a large number of potential slip surfaces in the slope. MCS method requires a lot of deterministic analysis for each possible slip surface, and the calculation cost is very high. The stochastic finite element method (SFEM) combining FEM with MCS method is an effective tool for reliability analysis of slope system. However, the computational efficiency of SFEM is low.

Under the framework of LEM, many scholars have proposed some methods that can effectively improve the computational efficiency of structural system reliability by reducing the sampling times of MCS method, such as the generalized subset simulation (GSS) method proposed by Yang [2], the WUS probability density weight method proposed by Ji [3], and the adaptive Monte Carlo simulation (AMCS) method proposed by Liu [4] and the PC-Kriging adaptive method proposed by Chen [5].

Studies have shown that not all failure modes have an important impact on the reliability of the structural system, and the failure probability of slope system is only determined by a few representative failure modes [6]. Based on this research conclusion, Zhang [7], Ji [8], Li [9], Li [10-11] proposed several slope system reliability calculation methods based on representative slip surfaces. Firstly, several representative slip surfaces which have important influence on the slope system

reliability are identified. Then, based on these representative slip surfaces, the slope system reliability is calculated by the structural system reliability calculation method.

However, in the above reliability calculation methods of slope system based on limit equilibrium, it is generally assumed that the potential slip surfaces are all circular, and performance functions are expressed by safety factor. It has shown that the shape of the slip surface has a significant effect on the calculation results of slope system reliability [12]. For homogeneous cohesive soil slope, the circular slip surface is realistic. While, for the case of complex soil distribution or weak interlayer, the real slip surface is usually non-circular. In addition, the characteristics of non-convex, non-smooth and nonlinear implicit functions of the safety factor determine the difficulty of its calculation process. Therefore, it is urgent to find a slope system reliability calculation method that can consider the general shape slip surface, the calculation process is simple, the accuracy meets the engineering requirements and the efficiency is high.

Chen [13] proposed a method for calculating the slope reliability of a single slip surface by using the explicit expression of the critical horizontal acceleration coefficient K_c as the performance function. The results show that the method not only has high accuracy, but also can significantly improve the computational efficiency. This study extends this method from a single slip surface to a slope system with multiple slip surfaces.

At present, the calculation methods of structural system reliability based on representative failure modes mainly include interval estimation method [14], product of conditional marginal (PCM) method [15], n-dimensional equivalent plane method [16], matrix-based system reliability (MSR) method [17] and sequential compounding method (SCM) [18]. The calculation results obtained by the interval estimation method are range values, which are not accurate enough. For highly nonlinear series systems, such as slopes, the PCM method is unstable, the n-dimensional equivalent plane method is not fully applicable, and the MSR method is not efficient. SCM can combine complex systems into a single component, which is suitable for parallel, series and hybrid systems. It is an ideal method for calculating the slope system reliability. Liao [19] successfully applied this method to the reliability analysis of

slope systems.

Rosenblueth method can realize the simple and efficient calculation of slope reliability index by selecting special calculation points [20]. Using this method to set the special combination of soil parameters is bound to improve the efficiency of slope system reliability calculation. Zhu [21] proposed the global critical slip field (GCSF) method, which does not need to assume the initial slip surface. It can accurately and quickly determine the critical slip surface of any shape, and the calculation results are stable and unique.

Based on the rigorous limit equilibrium method of normal stress correction of slip surface, considering the general shape of slip surface, the performance function adopts the explicit expression of critical horizontal acceleration coefficient K_c. By coupling Rosenblueth sampling point method, GCSF method and SCM, an efficient calculation method of slope system reliability is proposed. Firstly, the Rosenblueth sampling point method is used to set the soil parameter combination, and the GCSF method is used to search the general shape slip surface under each combination. Then, the representative slip surface is identified by the probabilistic network evaluation technique (PNET) method. Finally, based on the representative slip surfaces, the reliability of slope system is calculated by SCM.

It should be noted that the spatial variability of geotechnical physical and mechanical parameters is one of the important uncertain factors affecting slope stability. Ignoring the spatial variability of soil parameters may lead to unconservative estimates of the failure probability [22]. The random field theory can be used to quantitatively characterize the spatial variability of soil parameters. It has realized the expansion from one-dimensional to multi-dimensional [23-24], stationary to non-stationary [25-26], isotropic to anisotropic [27]. Some valuable research results have been obtained [28-30]. However, the main purpose of this paper is to propose an efficient method that can quickly identify the main representative slip surfaces and easily calculate the slope system reliability. The uncertainty of soil shear strength parameters is simplified, and only the statistical uniform random variable model is used. Spatial variability is not considered in the proposed method for the time being, which will be the direction of further research.

2. Basic theoretic framework

2.1. Slope reliability calculation method

2.1.1. Performance function

Sarma (1973) proposed the idea of using the critical horizontal acceleration coefficient K_c as an alternative to the safety factor F_s to evaluate the slope stability [31]. As shown in Fig.1, the two-dimensional slope has a general shape slip surface $s(x)$ and a slope surface $g(x)$. It is assumed that a static horizontal seismic force KW (expressed by the product of the horizontal acceleration coefficient K and the self-weight W) is applied to the sliding body. Based on the normal stress correction method over the slip surface, the equilibrium equations of the sliding body in the integral form can be listed, as shown in Equation (1). When the sliding body reaches the limit equilibrium state, that is, $F_s = 1$, the value of the horizontal acceleration coefficient K is K_c, as shown in Equation (2).
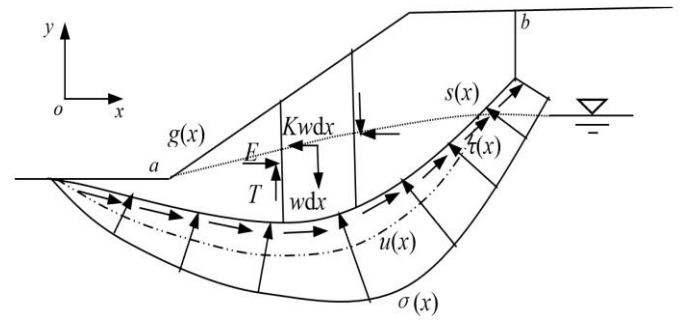

Figure 1. The force acting on the sliding body and the slice.

$$\int_a^b (-\sigma \cdot s' + \tau)\, dx - \int_a^b Kw\, dx = 0 \tag{1a}$$

$$\int_a^b (\sigma + \tau \cdot s')\, dx - \int_a^b w\, dx = 0 \tag{1b}$$

$$\int_a^b \left[w(x - x_c) + Kw\left(y_c - \frac{s+g}{2}\right) \right] dx - \int_a^b [(-\sigma \cdot s' + \tau)(y_c - s) + (\sigma + \tau \cdot s')(x - x_c)]\, dx = 0 \tag{1c}$$

where $s' = \frac{ds}{dx} = \tan\alpha$, α is the dip angle of the slip surface at x. (x_c, y_c) is the sliding mass center.

$$K_c = \frac{\lambda_1(A_1 + A_1') + \lambda_2(A_2 + A_2') - A_3'}{\lambda_2(B_1 + B_1') + \lambda_2(B_2 + B_2') - B_3'} \tag{2}$$

Where

$$\lambda_1 = \frac{G_3(B_2 + B_2') - G_2(A_3 + B_3')}{G_1(B_2 + B_2') - G_2(B_1 + B_1')} \tag{3a}$$

$$\lambda_2 = \frac{G_1(A_3 + B_3') - G_3(B_1 + B_1')}{G_1(B_2 + B_2') - G_2(B_1 + B_1')} \tag{3b}$$

$$G_1 = E_4(A_1 + A_1') - A_3(E_1 + D_1) \tag{3c}$$

$$G_2 = E_4(A_2 + A_2') - A_3(E_2 - D_2) \tag{3d}$$

$$G_3 = A_4 E_4 - A_3 E_3 + A_4' E_4 - A_3 D_3 \qquad (3e)$$

The detailed parameters in Equations (2-3) are as shown in Table 1.

Table 1. Detailed parameters description.

Detailed parameters		
$A_1 = -\int_a^b \sigma_0(x)\zeta_1(x)s' \, \mathrm{d}x$	$A_2 = -\int_a^b \sigma_0(x)\zeta_2(x)s' \, \mathrm{d}x$	$A_3 = \int_a^b w \, \mathrm{d}x$
$A_1' = \int_a^b \sigma_0(x)\zeta_1(x)\tan\varphi \, \mathrm{d}x$	$A_2' = \int_a^b \sigma_0(x)\zeta_2(x)\tan\varphi \, \mathrm{d}x$	$A_3' = \int_a^b (u\tan\varphi - c) \, \mathrm{d}x$
$B_1 = \int_a^b \sigma_0(x)\zeta_1(x) \, \mathrm{d}x$	$B_2 = \int_a^b \sigma_0(x)\zeta_2(x) \, \mathrm{d}x$	
$B_1' = \int_a^b \sigma_0(x)\zeta_1(x)s'\tan\varphi \, \mathrm{d}x$	$B_2' = \int_a^b \sigma_0(x)\zeta_2(x)s'\tan\varphi \, \mathrm{d}x$	$B_3' = \int_a^b (u\tan\varphi - c)s' \, \mathrm{d}x$
$D_1 = \int_a^b \sigma_0(x)\zeta_1(x)r_\tau(x)\tan\varphi \, \mathrm{d}x$	$D_2 = \int_a^b \sigma_0(x)\zeta_2(x)r_\tau(x)\tan\varphi \, \mathrm{d}x$	$D_3 = \int_a^b (u\tan\varphi - c)r_\tau(x) \, \mathrm{d}x$
$E_1 = \int_a^b \sigma_0(x)\zeta_1(x)r_\sigma(x) \, \mathrm{d}x$	$E_2 = \int_a^b \sigma_0(x)\zeta_2(x)r_\sigma(x) \, \mathrm{d}x$	$E_3 = \int_a^b w(x - x_c) \, \mathrm{d}x$
$E_4 = \int_a^b w\left(y_c - \dfrac{s+g}{2}\right) \, \mathrm{d}x$	$r_\sigma(x) = -s'(y_c - s) + x - x_c$	$r_\tau(x) = y_c - s + s'(x - x_c)$
$\sigma_0(x) = \dfrac{w}{1 + s'^2}$	$\zeta_1(x) = \dfrac{x-b}{a-b}$	$\zeta_2(x) = \dfrac{x-a}{b-a}$

The calculation formula of K_c is explicit and does not need to be solved iteratively. It is suitable for slip surface of any shape, and there is no problem that the calculation results do not converge [32]. In this paper, Equation (4) is used as the performance function for the reliability calculation of slope system.

$$Z = K_c - K_{c0} \qquad (4)$$

where K_{c0} is the known seismic coefficient. When there is no seismic load on the slope, K_{c0} is equal to zero.

2.1.2. Reliability calculation

It is assumed that the n-dimensional random variable affecting the slope stability is $\mathbf{X} = \{X_1, X_2, \cdots, X_n\}$, the slope failure probability can be expressed as

$$P_f = P(K_c(x) < K_{c0}) = \int_{K_c(X_i) < K_{c0}} f_{\mathbf{X}}(x)\mathrm{d}x \qquad (5)$$

where $f_x(x)$ is the probability density function of random variables.

Slope failure is generally a small failure probability event. The computational efficiency of MCS method is very low. The subset simulation (SS) method is an effective method to solve the problem of small failure probability [33]. In this paper, the SS method is used to calculate the slope failure probability.

The reliability index β can be calculated by the inverse function of the standard normal distribution function in Equation (6):

$$\beta = \Phi^{-1}(1 - P_f) \qquad (6)$$

where $\Phi^{-1}(x)$ is the inverse function of the standard normal distribution function.

2.2. Representative slip surface of general shape

Slopes have a large number of possible slip surfaces, and the shapes of these slip surfaces are usually not circular. Only a few slip surfaces have significant impacts on the calculation results of slope system reliability, which are called representative slip surfaces. On the basis of representative slip surfaces, the time consumption of calculating the slope system reliability is less. Considering the general shape of the slip surface, a representative slip surface identification method is proposed by coupling the Rosenblueth sampling point method, the GCSF method and the PNET method.
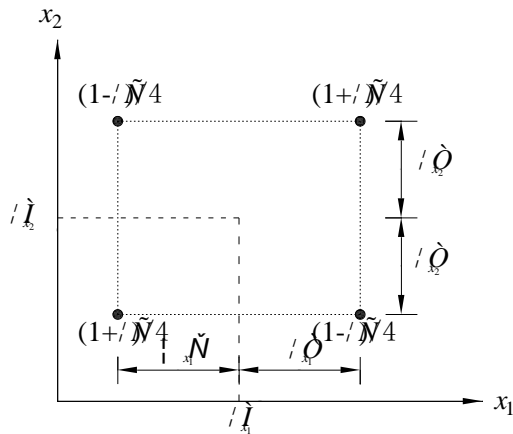
2.2.1. Rosenblueth sampling point method

Rosenblueth [34] proposed a point estimation method for approximating the lower moments of random variable functions. Chen [20] evaluated it as a simple, practical and accurate reliability calculation method. The high accuracy of Rosenblueth method benefits from its special calculation point selection method, which is called Rosenblueth sampling point

method here. This method is briefly introduced as follows.

When the mean and standard deviation of the random variable x_i ($i=1,2,\cdots,n$) are known, two sampling points with a standard deviation distance from the mean can be symmetrically selected, that is :
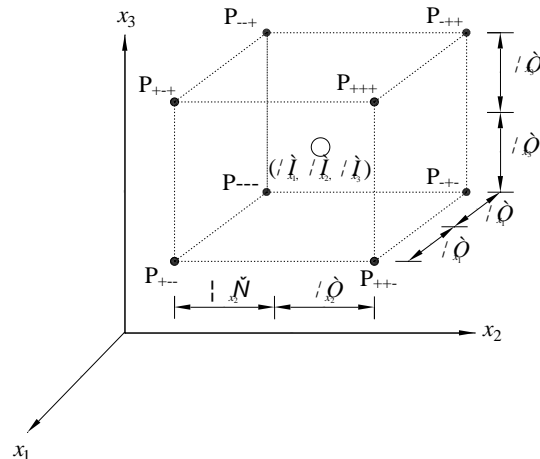
$$x_{i_1} = \mu_{x_i} + \sigma_{x_i} \qquad (7a)$$

$$x_{i_2} = \mu_{x_i} - \sigma_{x_i} \qquad (7b)$$

If the two random variables are x_1 and x_2, the rectangular coordinate system is established with them as the coordinate axis. The four sampling points set by the Rosenblueth method correspond to the four corner points of the rectangle, as shown in Figure 2(a).

(a) Two random variables   (b) Three random variables

Figure 2. Rosenblueth sampling points and weights of random variables.

While the number of random variables is 3, the eight sampling points set by the Rosenblueth method are the eight corners of the cuboid in the three-dimensional rectangular coordinate system, as shown in Figure 2(b).

In order to ensure the high accuracy of the reliability calculation results of the slope system, the Rosenblueth sampling point method is used to set 2^n combinations of soil random variable parameters.

2.2.2. Global critical slip field (GCSF) method

For the heterogeneous slope with large differences in soil parameters, the slip surface is generally not circular. However, considering the general shape of slip surface, the calculation process of slope system reliability is complicated.

The critical sliding field (CSF) method is based on the principle of maximum inter-slice thrust, that is, there is only one optimal path at any point in the slope to maximize its thrust. This method uniformly discretizes the slope into many state points, as shown in Figure 3. Taking the maximum thrust as the goal, the dangerous sliding direction of each state point is obtained. The dangerous sliding directions of all state points constitute the dangerous sliding field of the slope. Starting from the outlet state point of the slip surface with the largest residual

thrust, the critical slip surface is obtained by reverse tracking. The critical slip surfaces of all outlet state points constitute the global critical slip field (GCSF), as shown in Figure 4. The specific steps of this method can be found in Reference [21].
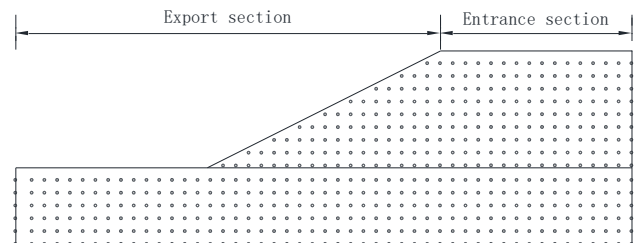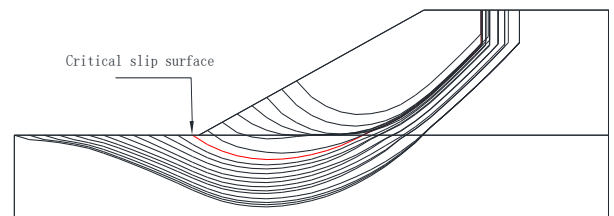

Figure 3. Discrete state points.

Figure 4. Global critical slip field (GCSF).

The GCSF method does not need to assume the initial slip surface. It can quickly and accurately determine the critical slip surface of any shape, and the calculation results are stable and unique. In this paper, the GCSF method is used as the search method of general shape slip surfaces.

2.2.3. Identification method of representative slip surface

According to the Rosenblueth sampling point method, 2^n parameter combinations are set, and 2^n critical slip surfaces can be searched by the GCSF method. The same sedimentary history and other factors make the soil parameters have a certain correlation, so these critical slip surfaces may also have some correlation [35]. On the basis of the reliability index of each slip surface and the correlation coefficient between the slip surfaces, the PNET method can be used to identify the representative slip surfaces.

2.2.3.1. Correlation analysis between slip surfaces

Chowdhury and Xu [36] introduced a correlation coefficient to measure the correlation between failure modes, and proposed an approximate calculation method. For the k th and l th failure modes, the approximate correlation coefficient can be calculated by Equation (8).

$$\rho_{kl} = \frac{\sum_{j=1}^{m} \frac{\partial Z_k}{\partial x_j} \frac{\partial Z_l}{\partial x_j} \sigma_{x_j}^2}{\sqrt{\sum_{j=1}^{m} \left(\frac{\partial Z_k}{\partial x_j}\sigma_{x_j}\right)^2} \sqrt{\sum_{j=1}^{m} \left(\frac{\partial Z_l}{\partial x_j}\sigma_{x_j}\right)^2}} \tag{8}$$

Where ρ_{kl} is the correlation coefficient between the kth and lth failure modes; Z_k and Z_l are the performance functions of the k th and l th failure modes, respectively, and m is the number of random variables. The partial derivatives of Z_k and Z_l to the random variable x_j are:

$$\frac{\partial Z_k}{\partial x_j} = \frac{z_k^+ - z_k^-}{2\sigma_{x_j}} \tag{9a}$$

$$\frac{\partial Z_l}{\partial x_j} = \frac{z_l^+ - z_l^-}{2\sigma_{x_j}} \tag{9b}$$

where Z_k^+, Z_k^-, Z_l^+ and Z_l^- are the performance function values obtained by increasing or decreasing a standard deviation σ_{x_j} on the basis of the mean of the corresponding random variables for the k th and l th failure modes, respectively.

2.2.3.2. Identification steps of representative slip surface

Probabilistic network evaluation technique (PNET) is widely used to identify representative failure modes. The main identification steps of representative slip surface using Rosenblueth sampling point method and GCSF method are as follows:

(1) The reliability indexes of 2^n critical slip surfaces searched by the GCSF method are calculated by the SS method.

(2) Find out the critical slip surface of the smallest reliability

index as the first representative slip surface;

(3) The correlation coefficients between the representative slip surface and other residual critical slip surfaces are calculated.

(4) The slip surfaces whose correlation coefficient ρ with the representative slip surface is greater than the threshold ρ_0 are excluded.

(5) The critical slip surface of the smallest reliability index is found among the remaining slip surfaces as a new representative slip surface.

(6) Repeat Steps 3-5 until no new representative slip surface can be found.

At present, the value of the correlation coefficient threshold has not yet formed a unified conclusion. Most studies take it as 0.8 or 0.9 [9,11,37]. Here, the correlation coefficient threshold is assumed to be 0.9.

2.4. Sequential compounding method (SCM)

The principle of SCM is to compound two components into a composite component in a certain order through the logical operation of union or intersection, until the complex system is finally compounded into a total component. This method can be conveniently applied to the reliability calculation of slope system.

Assuming that a slope has N_r representative slip surfaces (S_1, S_2,... S_{Nr}), it can be regarded as a series system composed of N_r components. S_1 and S_2 can be combined into an equivalent element S_{1or2} by SCM. Then S_{1or2} is further compounded with component S_3. All components are eventually compounded into an equivalent total component $S_{(1or2or...orNr)}$, as shown in Figure 5. According to the above ideas, the failure probability of the slope system can be expressed by Equation (10).

$$P_{\text{fsys}} = P\big[E(S_1) \cup E(S_2) \cdots \cup E(S_{N_r})\big] = P\big[E(S_{1or2}) \cup E(S_3) \cdots \cup E(S_{N_r})\big] \tag{10}$$

where $E(S_i)$ denotes the event of slope failure along the i-th slip surface, $i = 1,2,\cdots, N_r$; P [•] is the failure probability of the event.
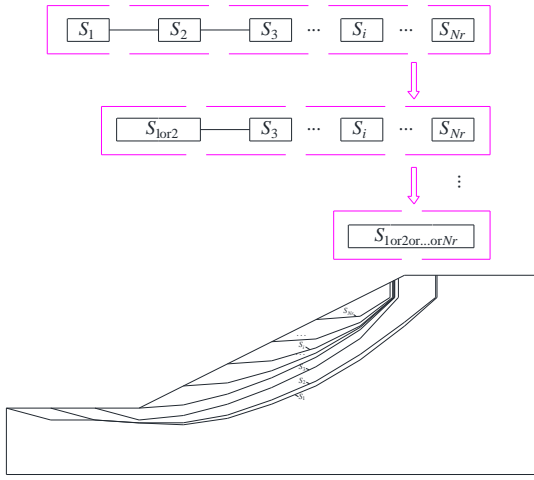
Figure 5. Schematic diagram of sequential compounding method.

Since there is a one-to-one correspondence between the reliability index and the failure probability, the reliability index of the equivalent component S_{1or2} can be calculated by Equation (11) [18]:

$$\beta_{1or2} = -\Phi^{-1}[P_{f(1or2)}] = -\Phi^{-1}[\Phi(-\beta_1) + \Phi(-\beta_2) - \Phi_2(-\beta_1, -\beta_2; \rho_{1,2})] \quad (11)$$

where $\Phi_2(\cdot)$ is a two-dimensional standard normal cumulative distribution function; $\rho_{1,2}$ is the correlation coefficient between S_1 and S_2. β_1, β_2 and P_{f1}, P_{f2} are their reliability index and failure probability, respectively.

$\Phi_2(-\beta_1, -\beta_2; \rho_{1,2})$ in Equation (11) can be approximately solved by using normal distribution function after dimension reduction by conditional probability.

$$\Phi_2(-\beta_1, -\beta_2; \rho_{1,2}) = P(Z_1 < -\beta_1 | Z_2 < -\beta_2)P(Z_2 < -\beta_2) \approx F_{Z_1 < -\beta_1 | Z_2 < -\beta_2}(-\beta_1)\Phi(-\beta_2) = \Phi(-\beta_{1|2})\Phi(-\beta_2) \quad (12)$$

where $\beta_{1|2}$ is the condition reliability index of S_1 under the condition of S_2 failure, which can be calculated by Equation (13):

$$\beta_{1|2} = \frac{\beta_1 - \rho_{1,2}A_2}{\sqrt{1 - \rho_{1,2}^2 B_2}} \quad (13a)$$

$$A_2 = \frac{\phi(-\beta_2)}{\Phi(-\beta_2)} \quad (13b)$$

$$B_2 = A_2(-\beta_2 + A_2) \quad (13c)$$

where $\phi(\cdot)$ is the standard normal probability density function.

Substituting Equations (12) - (13) into Equation (11), we can get:

$$\beta_{1or2} = -\Phi^{-1}[\Phi(-\beta_1) + \Phi(-\beta_2) - \Phi(-\beta_{1|2})\Phi(-\beta_2)] \quad (14)$$

Similarly, when S_{1or2} is compounded with S_i, under the condition of S_i failure, the conditional reliability index $\beta_{(1or2)|i}$ can be expressed by Equations (15-16):

$$\beta_{(1or2)|i} = -\Phi^{-1}[\Phi(-\beta_{1|i}) + \Phi(-\beta_{2|i}) - \Phi_2(-\beta_{1|i}, -\beta_{2|i}; \rho_{1,2|i})] \quad (15)$$

$$\beta_{(1or2)|i} = \frac{\beta_{1or2} - \rho_{(1or2),i}A_i}{\sqrt{1 - \rho_{(1or2),i}^2 B_i}} \quad (16)$$

where

$$\beta_{1|i} = \frac{\beta_1 - \rho_{1,i}A_i}{\sqrt{1 - \rho_{1,i}^2 B_i}} \quad (17a)$$

$$\beta_{2|i} = \frac{\beta_2 - \rho_{2,i}A_i}{\sqrt{1 - \rho_{2,i}^2 B_i}} \quad (17b)$$

$$\rho_{(1or2)|i} = \frac{\rho_{1,2} - \rho_{1,i}\rho_{2,i}B_i}{\sqrt{1 - \rho_{1,i}^2 B_i}\sqrt{1 - \rho_{2,i}^2 B_i}} \quad (17c)$$

$$A_i = \frac{\phi(-\beta_i)}{\Phi(-\beta_i)} \quad (17d)$$

$$B_i = A_i(-\beta_i + A_i), (i = 3,4,\cdots,N_r) \quad (17e)$$

By solving Equations (15) and (16) simultaneously and limiting the range of $\rho_{(1or2),i}$ in [-1,1], we can obtain its value. It should be noted that selecting components according to the ascending order of reliability index will make the calculation results more accurate.

3. Reliability calculation method of slope system with general shape slip surface

Combined with Rosenblueth sampling point method, GCSF method, SCM and PNET method, an efficient calculation method of slope system reliability is proposed. In this method, the Rosenblueth sampling point method is used to construct 2^n random variable parameter combinations, and the GCSF method is used to search the slip surface of each parameter combination. The slip surface with the smallest safety factor in each combination is selected as the critical slip surface, and its reliability index is calculated by the method in Reference [13]. Then the representative slip surfaces are identified by the PNET method, and the reliability index of slope system is calculated by SCM.

The flow chart of the above efficient method for calculating system reliability of soil slope with general shape slip surfaces is illustrated in Figure 6.
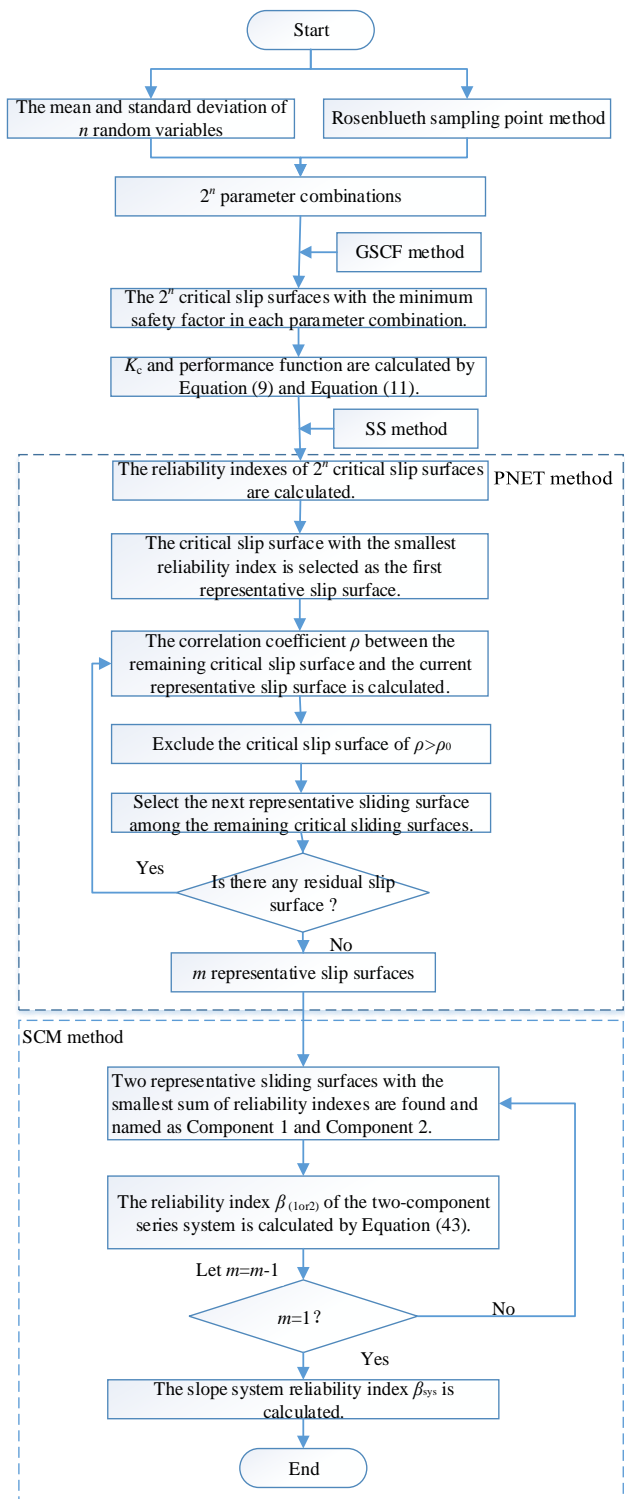
Figure 6. Flow chart of efficient calculation method of slope system reliability.

4. Examples Studies

4.1. Example 1

Example 1 is a slope composed of two cohesive soil layers

designed by Ching (2009) [38], as shown in Figure 7. The undrained shear strength parameters of the two soil layers are independent of each other and obey the lognormal distribution, and the coefficient of variation is 0.3, as shown in Table 2. Some scholars assume that the slip surfaces are all circular, and use different methods to analyze the reliability of the slope system, such as Ching [38], Low [39], Ji [3], Cho [40], Kang [41], Yang [2], and Ji [8].

In order to study the influence of the shape of the slip surface on the calculation results, the reliability of slope system is calculated by considering circular and non-circular slip surfaces respectively. Geo-studio software is used to search the circular slip surfaces.

Table 2. Soil layer parameters of Example 1.

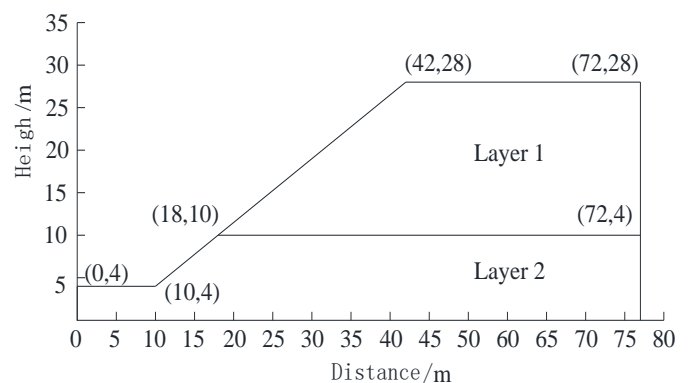| Soil layers	c(kPa)		γ(kN/m^3)	Distribution
	μ_c	σ_c		
1	120	36	19	Lognormal
2	160	48	19	Lognormal

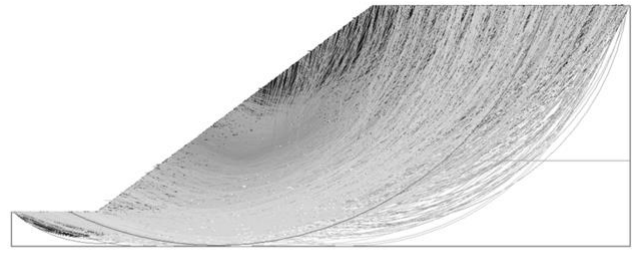Figure 7. The slope section of Example 1.

4.1.1. Circular slip surface

According to the mean and standard deviation of undrained shear strength parameters c_1 and c_2 in Table 2, four parameter combinations are generated by Equation (7a) ~ (7b). For each combination, 5000 circular slip surfaces are searched by Geo-studio software, as shown in Figure 8 (a) - (d).
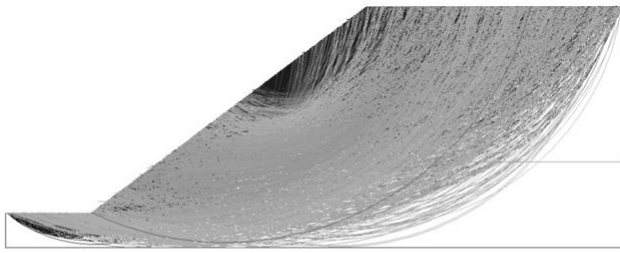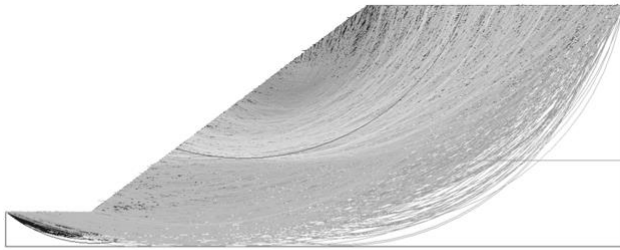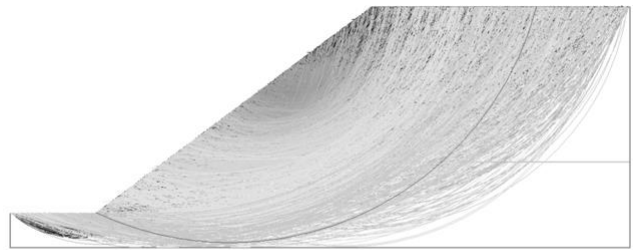
(a) c_1=156kPa, c_2=208 kPa

(b) c_1=156 kPa, c_2=112 kPa

(c) c_1=84 kPa, c_2=208 kPa

(d) c_1=84 kPa, c_2=112 kPa

Figure 8. The circular slip surfaces under different parameter combinations in Example 1.

The critical slip surface with the smallest safety factor in each group of slip surfaces is named Slip surface 1-4 (hereinafter referred to as S1-S4), where S1 and S4 overlap, as shown in Figure 9.

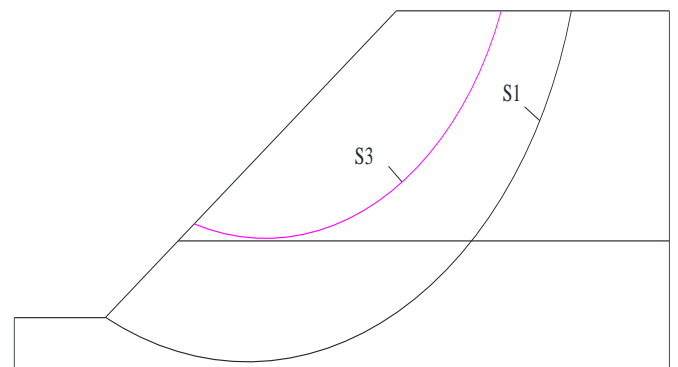Figure 9. Four circular critical slip surfaces in Example 1.

Using the efficient calculation method of slope reliability based on rigorous limit equilibrium, the reliability indexes of these four critical slip surfaces are obtained: $\beta_1=\beta_4$=3.0037, β_2=3.1426, β_3=2.7944. Among them, the reliability index of S3 is the smallest, which can be used as the first representative slip surface. The correlation coefficients between the three slip surfaces calculated by Equation (8) are: ρ_{12}=1.000, ρ_{13}=0.348, ρ_{23}=0.331. Both ρ_{13} and ρ_{23} are less than the threshold ρ_0 (ρ_0=0.9), so no slip surface is excluded. Among the remaining slip surfaces, the slip surface S1 with the smallest reliability index is used as the second representative slip surface. Since ρ_{12} is greater than ρ_0, S2 can be excluded. So far, all representative slip surfaces have been found, as shown in Figure 10.

Figure 10. Two circular representative slip surfaces in Example 1.

Since the reliability index of S3 is less than that of S1, the slip surfaces S3 and S1 can be named as Component 1 and Component 2, respectively. The reliability index of the composite component calculated by Equation (14) is $\beta_{(1or2)}$=2.6636. There are only two representative slip surfaces in this example, so the reliability index of the slope system is β_{sys}=2.6636. According to the standard normal distribution function, the failure probability of the slope system can be calculated as P_{fsys} = 0.0039.

The slope system reliability results of Example 1 calculated by different methods are listed in Table 3.

Table 3. System reliability calculation results of different methods in Example 1.

Method of analysis	Sampling number	System failure probability P_{fsys}	Reference
MCS	10,000	0.0044	Ching (2009) [38]
IS	1,000	0.0041	Ching (2009) [38]
SA		{0.0043,0.0044}	Low (2011) [39]
FORM+SRSM		{0.0040,0.0041}	Ji (2012) [8]
MCS+SRSM	50,000	0.0039	Ji (2012) [8]
MCS	20,000	0.0042	Cho (2013) [40]
MCS + SVM	100,000	0.0040	Kang (2016) [41]
GSS	1643	0.0044	Yang (2018) [2]
WUS	500	0.0042	Ji (2021) [3]
SS+SCM	5,000	0.0039	This study

Note：MCS - Monte Carlo simulation；IS-Importance sampling；SA-Spreadsheet algorithm； FORM-First-order reliability method；SRSM-Stratified response surfaces method； SVM-Support vector machine；SS-Subset simulation；SCM-Sequential compounding method.

It can be seen from Table 3 that the system reliability calculation result of this method is very close to those of FORM + SRSM method, MCS + SRSM method, IS method and MCS + SVM method, and is slightly smaller than those of MCS method, WUS method, SA and GSS method.

4.1.2. Non-circular slip surface

When the soil parameters are taken as the mean value, considering that the slip surface is non-circular, the safety factor of the critical slip surface searched by GCSF method is 1.810, which is less than 1.863 of Morgenstern-Price method in Geo-studio software. It is also less than the minimum safety factor of 2.003 in the case of circular slip surface. It can be seen that the GCSF method can obtain a non-circular slip surface with a smaller safety factor than that of the circular slip surface.

Considering the non-circular slip surface, the dangerous slip surfaces searched in four combinations are shown in Figure 11.

(a) c_1=156kPa, c_2=208 kPa

(b) c_1=156 kPa, c_2=112 kPa

(c) c_1=84 kPa, c_2=208 kPa
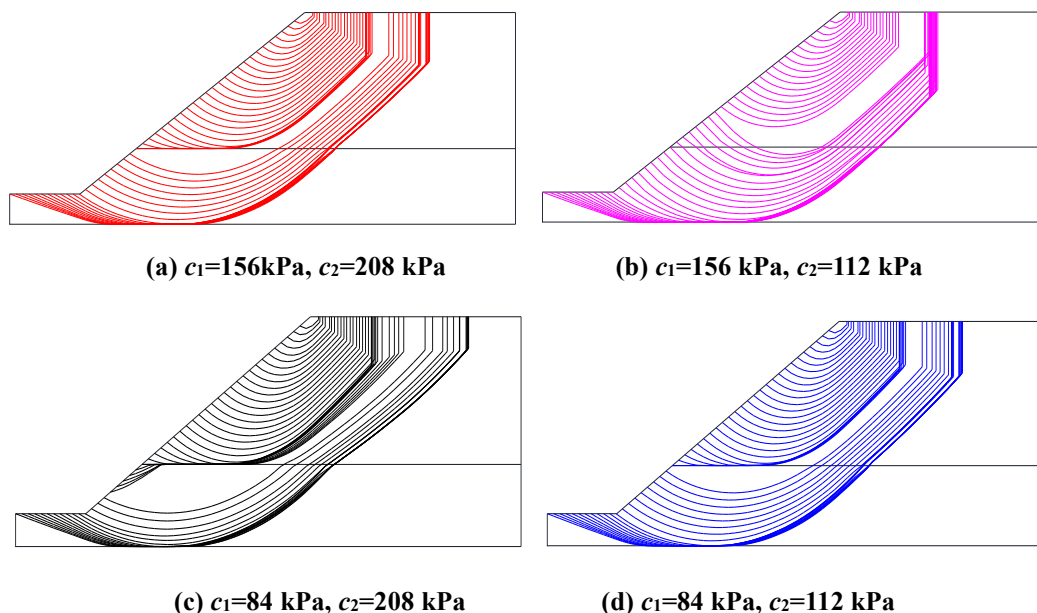

(d) c_1=84 kPa, c_2=112 kPa

Figure 11. The non-circular slip surfaces under different parameter combinations in Example 1.

The critical slip surfaces with the smallest safety factor in the four groups of dangerous slip surfaces are named as S1-S4, as shown in Figure 12. Among them, S1 and S4 still overlap. The reliability indexes of these four slip surfaces are:

β_1=β_4=2.3199, β_2= 2.2451, β_3=2.6203.

The reliability index of S2 is the smallest, which can be used as the first representative slip surface. The correlation coefficients of S2 with S1 and S3 are ρ_{12}=0.991 and ρ_{23}=0.177,

respectively. Because $\rho_{12}>\rho_0$, S1 can be excluded, and the representative slip surfaces are S2 and S3, as shown in Figure 13.
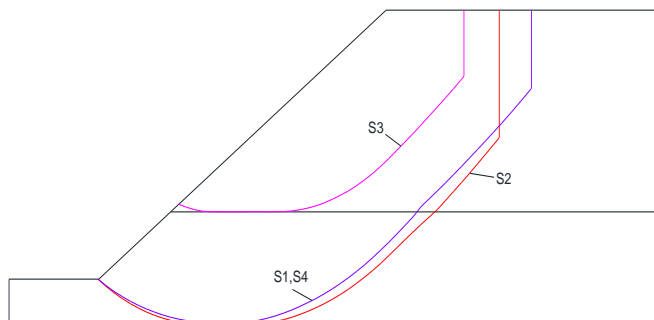

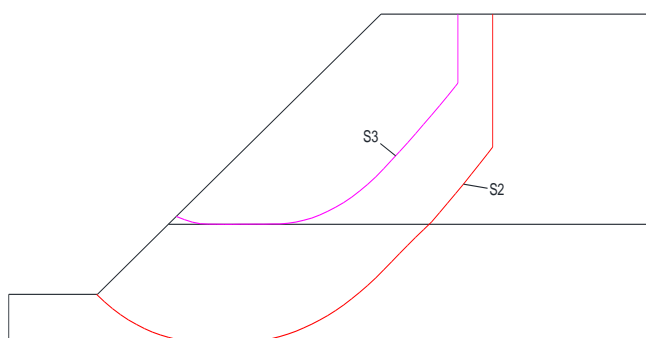Figure 12. Four non-circular critical slip surfaces of Example 1.

Figure 13. Two non-circular representative slip surfaces of Example 1.

According to the ascending order of reliability index, S2 and S3 are named Component 1 and Component 2 respectively. The system failure probability is calculated to be P_{fsys}= 0.0166, which is about 4 times of the calculation result considering the circular slip surface. It can also be seen that the non-circular slip surface searched by the GCSF method is more dangerous than the circular slip surface, and the failure probability of the slope system is also greater.

In order to compare the positions of the slip surfaces more intuitively, the circular and non-circular representative slip surfaces obtained by the proposed method and that in the references are drawn in Figure 14. It can be seen from Figure 14 that the position of the non-circular slip surface is close to those of the circular slip surfaces in this study and references, except for some differences at the entrance of the slip surface. The main reason for the difference is that the GCSF method considers the non-tensile properties of geotechnical materials, and sets tensile cracks at the positions where the tensile stress is greater than zero to eliminate it. Studies have shown that the tensile-shear

combined failure surface can often obtain a smaller safety factor than the pure shear failure surface [42]. This is also one of the reasons why the reliability of the slope system calculated by the proposed method is greater than that of the traditional method considering the circular slip surface.
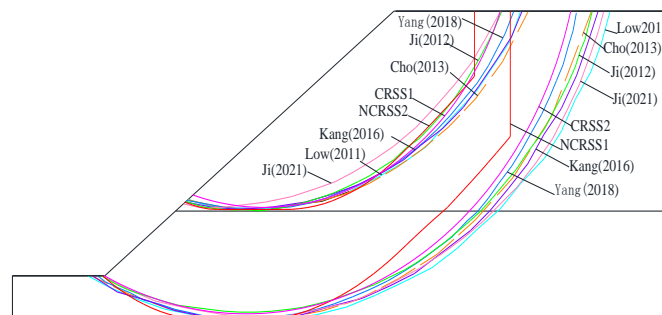

Figure 14. Comparison of representative slip surface of Example 1.
(CRSS-Circular representative slip surface; CRSS-Non-circular representative slip surface)

In order to verify the accuracy of the calculation results of this method in the case of non-circular slip surface, the Geo-studio software was used to calculate the system reliability of Example 1. A total of 275 slip surfaces were obtained, as shown in Figure 15. The MCS method was used to calculate the reliability of the slope system with 25,000 samples. The system failure probability is P_{fsys}=0.0170, and the reliability index is β_{sys}=2.1114. The errors between the proposed method and the MCS method are -2.35 % and 0.73 %, respectively. This shows that the proposed calculation method is effective.
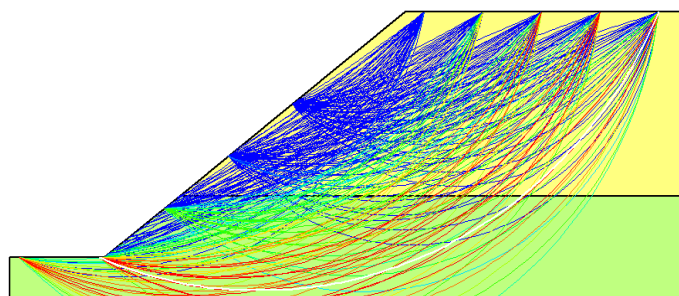

Figure 15. The slip surfaces of Geo-studio in Example 1.

The CPU time of the proposed method is 184 seconds, while that of the Geo-studio software using the MCS method is 3498 seconds, which is about 19 times that of this method. Therefore, this method is a reliability calculation method of slope system which can achieve high precision and high efficiency at the same time.

4.2. Example 2

Example 2 is selected from a slope stability test problem of the Australian Computer Application Society (ASCDS) [43]. The slope contains a weak interlayer with a thickness of 0.5 m, and the distribution of soil layer is shown in Figure 16. The material parameters of each soil layer are listed in Table 4. The safety factor of the critical slip surface obtained by GCSF method is 1.215, which is less than 1.240 of ACADS [43], 1.241 of Cheng et al [44] and 1.230 of Liu [4].
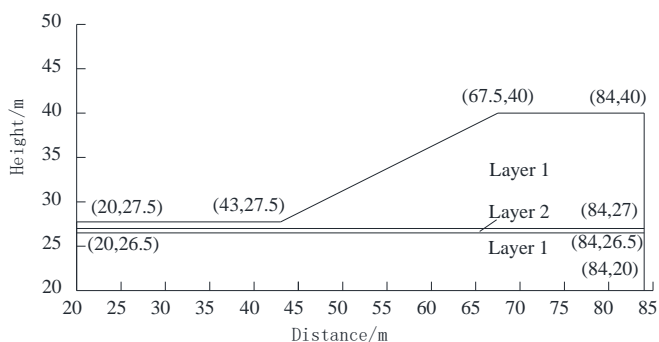
Table 4. Soil parameters of Example 2.

Soil layers	c(kPa)		φ (°)		γ(kN/m³)	Distribution
	μ_c	σ_c	μ_φ	σ_φ		
1	28.5	8.55	20	6	18.84	Normal
2	0	0	10	2	18.84	Normal

Note: In Soil layer 2, μ_c=0, σ_c=0, that is, the soil is non-cohesive, the cohesion is very small and can be ignored.

According to the mean and standard deviation of random variables c_1, φ_1 and φ_2, eight parameter combinations (37.05, 26, 12), (37.05, 26, 8), (37.05, 14, 12), (37.05, 14, 8), (19.95, 26, 12), (19.95, 26, 8), (19.95, 14, 12) and (19.95, 14, 8) were generated by Rosenblueth sampling point method. For each combination, the GCSF method is used to search for 50 dangerous slip surfaces, as shown in Figure 17.

Figure 16. The slope section of Example 2.

(a) c_1=37.05kPa, φ_1=26°,φ_2=12°

(b) c_1=37.05kPa, φ_1=26°,φ_2=8°

(c) c_1=37.05kPa, φ_1=14°,φ_2=12°

(d) c_1=37.05kPa, φ_1=14°,φ_2=8°

(e) c_1=19.95kPa, φ_1=26°,φ_2=12°

(f) c_1=19.95kPa, φ_1=26°,φ_2=8°

(g) c_1=19.95kPa, φ_1=14°,φ_2=12°

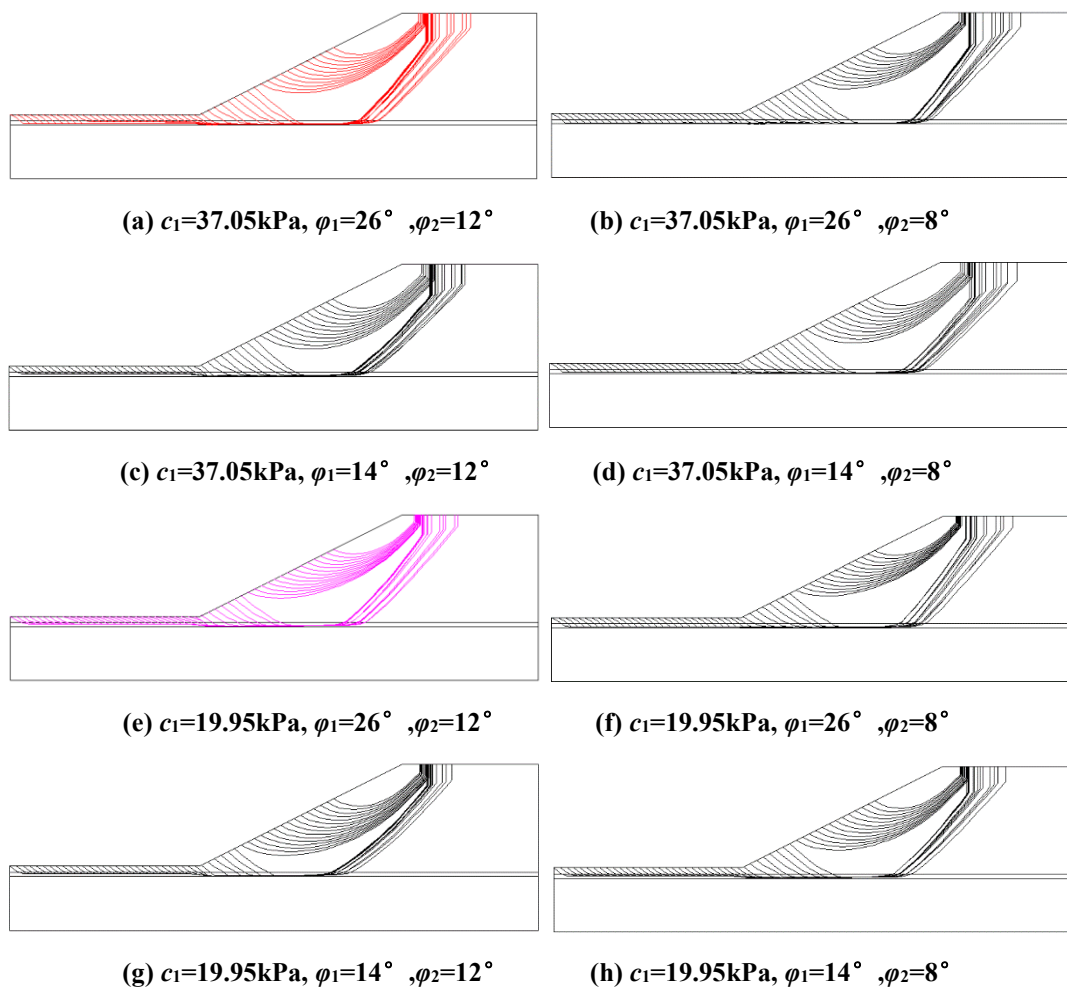**(h) c_1=19.95kPa, φ_1=14°,φ_2=8°**

Figure 17. The non-circular slip surfaces under different parameter combinations in Example 2.

The critical slip surfaces with the smallest safety factor are found in the eight groups of dangerous slip surfaces, which are named as S1-S8 in turn, as shown in Figure 18.
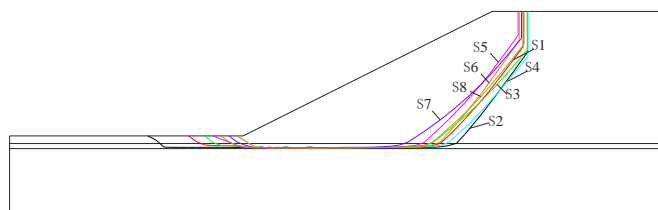

Figure 18. Eight critical slip surfaces of Example 2.

The reliability of these eight critical slip surfaces is calculated respectively, and the reliability indexes are obtained as follows: $\beta_1=1.4915$, $\beta_2=1.7669$, $\beta_3=1.3576$, $\beta_4=1.4939$, $\beta_5=1.5907$, $\beta_6=1.5965$, $\beta_7=1.3522$, $\beta_8=1.4352$. The correlation coefficient matrix between the eight slip surfaces is as shown in Table 5:

Table 5. The correlation coefficient matrix between the eight slip surfaces in Example 2.

ρ_{ij}	S1	S2	S3	S4	S5	S6	S7	S8
S1	1.000	0.987	0.988	0.997	0.985	0.999	0.961	0.961
S2	0.987	1.000	0.955	0.979	0.946	0.981	0.896	0.956
S3	0.988	0.955	1.000	0.995	0.990	0.990	0.989	0.998
S4	0.997	0.979	0.995	1.000	0.984	0.996	0.970	0.994
S5	0.985	0.946	0.990	0.984	1.000	0.991	0.989	0.996
S6	0.999	0.981	0.990	0.996	0.991	1.000	0.969	0.993
S7	0.961	0.896	0.989	0.970	0.989	0.969	1.000	0.990
S8	0.961	0.956	0.998	0.994	0.996	0.993	0.990	1.000

Among the eight slip surfaces, S7 has the smallest reliability index, so S7 is taken as the first representative slip surface. From Table 5, it can be seen that among these correlation coefficients between S7 and the other seven slip surfaces, only ρ_{72} is less than the threshold 0.9, that is, S2 is the second representative slip surface. The correlation coefficients between S2 and the remaining six slip surfaces are all greater than 0.9. At this time, no new representative slip surface can be selected. Therefore, there are only two representative slip surfaces in this example - S7 and S2, as shown in Figure 19. S7 and S2 are named as Component 1 and Component 2, and the reliability index and failure probability of the slope system are calculated to be 1.2853 and 0.0993 respectively.
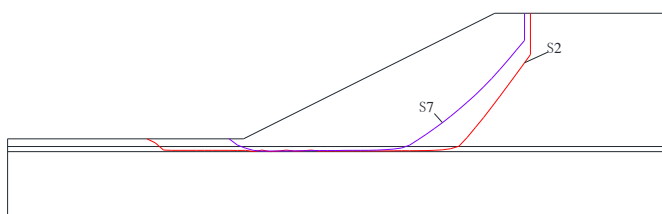

Figure 19. Two representative slip surfaces of Example 2.

In the Geo-studio software, the MCS method was used to calculate the slope reliability of 10,000 samples on 126 slip surfaces, and the reliability index and failure probability were

1.3432 and 0.0896. The critical slip surface is shown in Figure 20. The calculation results of the proposed method are close to those of Geo-studio, and the representative slip surface S7 with the smallest reliability index is also close to the critical slip surface of Geo-studio, as shown in Figure 21, which proves the effectiveness of this method.
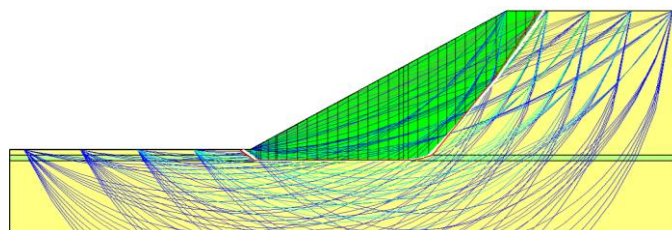

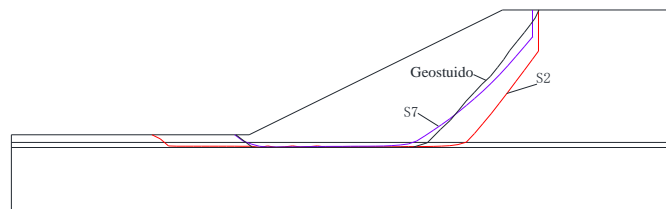Figure 20. The critical slip surface of Geo-studio in Example 2.

Figure 21. Comparison of slip surface results of Example 2.

In terms of computational efficiency, the CPU time of the MCS method in Geo-studio is 8664 seconds, while the computational time of the proposed method is only 322 seconds,

which is about 1/27 of the former, indicating the high efficiency of this method.

5. Conclusion

An efficient calculation method of slope system reliability considering general shape slip surface is proposed. The Rosenblueth point selection method is used to set the parameter combinations of random variables. The GCSF method is used to search for the critical slip surface of any shape under each combination. The slope reliability calculation method based on rigorous limit equilibrium is used to calculate the reliability indexes of these critical slip surfaces. The PNET method is used to identify the representative slip surfaces, and the SCM method is used to calculate the reliability of the slope system.

The calculation results of slope system reliability of two examples show that:

(1) The proposed method can quickly identify the main representative slip surfaces with only a small amount of calculation, and conveniently and effectively calculate the reliability index and failure probability of the slope system. Compared with the MCS method, this method has higher computational accuracy and efficiency.

(2) The shape of the slip surface has a significant effect on the reliability of the slope system. The GCSF method can be used to obtain a general-shaped critical slip surface with a greater failure probability than the traditional circular slip surface.

(3) The number of main representative slip surfaces identified based on the Rosenblueth sampling point method is small, and these slip surfaces can be used as reference slip surfaces for slope reinforcement design.

However, it should be noted that the proposed method only simply regards the soil parameters as random variables with known distribution characteristics, and does not consider their spatial variability. Spatial variability has a significant effect on the failure mode and reliability calculation results. Considering the spatial variability of soil parameters is the direction of further improvement of this method. In addition, the influence of rainfall and groundwater seepage on slope reliability is not taken into account. These external factors are often the main causes of slope instability. An efficient method for calculating the time-dependent reliability considering the influence of seepage will be used as a further extension of the proposed method.

References

1. Duncan J M. Factors of safety and reliability in geotechnical engineering. Journal of Geotechnical and Geoenvironmental Engineering 2000;126(4): 307–316. https://doi.org/10.1061/(ASCE) 1090-0241(2000)126:4(307).

2. Yang Z Y, Li D Q, Cao Z J, Tang X S. System reliability of soil slope using generalized subset simulation. Rock and Soil Mechanics 2018;39(3):957–966+984. https://doi.org/ 10.16285/j.rsm.2016.0780.

3. Ji J, Wang L P, Liao W W, Zhang W J, Zhu D S, Gao Y F. System reliability analysis of slopes based on weighted uniform simulation method. Chinese Journal of Geotechnical Engineering 2021; 43(8): 1492–1501. https://doi.org/10.11779/CJGE202108014.

4. Liu X, Li D Q, Cao Z J, Wang Y. Adaptive Monte Carlo simulation method for system reliability analysis of slope stability based on limit equilibrium methods. Engineering Geology 2020;264: 105384. https://doi.org/10.1016/j.enggeo.2019.105384.

5. Chen P, Zhao C, Yao H, Zhao S. An adaptive method based on PC-Kriging for system reliability analysis of truss structures, Eksploatacja i Niezawodność – Maintenance and Reliability 2023;25(3): 169497. http://doi.org/10.17531/ein/169497.

6. Zhang J, Zhang L M, Tang W H. New methods for system reliability analysis of soil slopes. Canadian Geotechnical Journal 2011;48(7):1138–1148. https://doi.org/10.1139/t11-009

7. Zhang J, Huang H W, Juang C H, et al. Extension of Hassan and Wolff method for system reliability analysis of soil slopes. Eng Geol 2013; 160:81–88. https://doi.org/ 10.1016/j.enggeo.2013.03.029.

8. Ji J, Low B K. Stratified response surfaces for system probabilistic evaluation of slope. J Geotech Geoenviron 2012;138(11):1398–1406.

https://doi.org/10.1061/(ASCE)GT.1943-5606.0000711.

9. Li J P, Cheng Y G, Li D Q, Chang X L. System reliability analysis of spatially variable soil slopes using the multiple response surfaces method. Rock and Soil Mechanics 2016;37(1): 147–155+165. https://doi.org/10.16285/j.rsm.2016.01.018.

10. Li L, Wang Y, Cao Z. Probabilistic slope stability analysis by risk aggregation. Engineering Geology 2014;176: 57–65. https://doi.org/10.1016/j.enggeo.2014.04.010.

11. Li L, Chu X S. Locating the multiple failure surfaces for slope stability using monte carlo technique. Geotechnical and Geological Engineering 2016;34(5):1475-1486. https://doi.org/ 10.1007/s10706-016-0055-1.

12. Hassan A M, Wolff T F. Search algorithm for minimum reliability index of earth slopes. Journal of Geotechnical and Geoenvironmental Engineering, 1999, 125(4):301–308. doi: 10.1061/(ASCE) 1090-0241(1999)125:4(301).

13. Chen J X, Zhu D Y, Zhu Y L. An efficient method for computing slope reliability calculation based on rigorous limit equilibrium. Applied Rheology, 2023, 33(1): 20220147. doi: 10.1515/arh-2022-0147.

14. Ditlevsen O. Hallow reliability bounds for structural system. Journal of Structural Mechanics 1979;7(4):453–472. https://doi.org/10.1080/03601217908905329.

15. Pandey M D. An effective approximation to evaluate multinormal integrals. Structural Safety 1998; 20(1): 51–67. https://doi.org/10.1016/S0167-4730(97)00023-4.

16. Gollwitzer S, Rackwitz R. Equivalent components in first-order system reliability. Reliability Engineering 1983;5(2):99–115. https://doi.org/10.1016/0143-8174(83)90024-0.

17. Kang W H, Song J, Gardoni P. Matrix-based system reliability method and applications to bridge networks. Reliability Engineering & System Safety 2008;93(11): 1584–1593. https://doi.org/10.1016/j.ress.2008.02.011.

18. Lin X, Tan X H, Dong X L, Du L F, Zha F S, Xu L. System reliability sensitivity analysis method based on sequential compounding method. Chinese Journal of Geotechnical Engineering 2022;44(1):98–106. https://doi.org/10.11779/CJGE202201009.

19. Liao K, Wu Y P, Miao F S, et al. Efficient system reliability analysis for layered soil slopes with multiple failure modes using sequential compounding method. ASCE-ASME J. Risk Uncertainty Eng. Syst., Part A: Civ. Eng. 2023;9(2): 04023015. https://doi.org/10.1061/AJRUA6.RUENG-1022.

20. Chen Z Y, Du J F, Yan J J, et al. Point estimation method: Validation, efficiency improvement, and application to embankment slope stability reliability analysis. Engineering Geology 2019;263: 105232. https://doi.org/10.1016/j.enggeo.2019.105232.

21. Zhu D Y, Zhou Z S. Theory of globally critical slip field of slopes and its application to practical engineering. China civil engineering journal 1999;32(3):66–72. https://doi.org/10.3321/j.issn:1000-131X.1999.03.011.

22. Griffiths D, Fenton G A. Probabilistic slope stability analysis by finite elements. J Geotech Geoenviron 2004;130(5):507–518. https://doi.org/10.1061/(ASCE)1090-0241(2004)130:5(507).

23. Nguyen T S, Likitlersuang S, Tanapalungkorn W, Phan T N, Keawsawasvong S. Influence of copula approaches on reliability analysis of slope stability using random adaptive finite element limit analysis. International Journal for Numerical and Analytical Methods in Geomechanics 2022; 46(12), 2211-2232. https://doi.org/10.1002/nag.3385.

24. Nguyen T S, Tanapalungkorn W, Keawsawasvong S, Lai V Q, Likitlersuang S. Probabilistic analysis of passive trapdoor in c-ϕ soil considering multivariate cross-correlated random fields. Geotechnical and Geological Engineering 2024;42(3):1849–1869. https://doi.org/10.1007/s10706-023-02649-5.

25. Nguyen, T S, Likitlersuang S. Influence of the spatial variability of the root cohesion on a slope-scale stability model: a case study of residual soil slope in Thailand. Bulletin of Engineering Geology and the Environment 2019;78(5):3337-3351. https://doi.org/10.1007/s10064-018-1380-9.

26. Nguyen T S, Phan T N, Likitlersuang S, Bergado D T. Characterization of stationary and nonstationary random fields with different copulas on undrained shear strength of soils: Probabilistic Analysis of Embankment Stability on Soft Ground. International Journal of Geomechanics 2022;22(7): 04022109. https://doi.org/10.1061/(ASCE)GM.1943-5622.0002444.

27. Nguyen T S, Tanapalungkorn W, Likitlersuang S. Probabilistic Analysis of Dual Circular Tunnels in Rock Mass Considering Rotated Anisotropic Random Fields. Computers and Geotechnics 2024;170: 106319. https://doi.org/10.1016/j.compgeo.2024.106319.

28. Nguyen T S, Likitlersuang S. Reliability analysis of unsaturated soil slope stability under infiltration considering hydraulic and shear

strength parameters. Bulletin of Engineering Geology and the Environment 2019;78(8):5727-5743. https://doi.org/10.1007/s10064-019-01513-2.

29. Nguyen T S, Likitlersuang S. Influence of the spatial variability of soil shear strength on deep excavation: A Case Study of a Bangkok Underground MRT Station. International Journal of Geomechanics 2021; 21(2):04020248. https://doi.org/10.1061/(ASCE)GM.1943-5622.0001914.

30. Tanapalungkorn W, Yodsomjai W, Keawsawasvong S, et al. Undrained stability of braced excavations in clay considering the nonstationary random field of undrained shear strength. Scientific Report 2023;13:13358. https://doi.org/10.1038/s41598-023-40608-5.

31. Sarma S K. Stability analysis of embankments and slopes. Géotechnique 1973;23(3): 423–433. https://doi.org/10.1680/geot.1973.23.3.423.

32. Sarma S K, Bhave MV. Critical acceleration versus static factor of safety in stability analysis of earth dams and embankments. Géotechnique 1974;24(4): 661–665. https://doi.org/10.1680 /geot.1974.24.4.661.

33. Au S K, Wang Y. Engineering risk assessment with Subset Simulation. Singapore: John Wiley & Sons; 2014. https://doi.org/10.1002/9781118398050.

34. Rosenblueth E. Point estimates for probability moments. Proceedings of the National Academy of Sciences.1975,72 (10): 3812–3814. https://doi.org/10.1073/pnas.72.10.3812.

35. Zeng P, Jimenez R, Jurado-Pina R. System reliability analysis of layered soil slopes using fully specified slip surfaces and genetic algorithms. Engineering Geology 2015;193: 106–117. https://doi.org/10.1016/j.enggeo.2015.04.026.

36. Chowdhury R N, Xu D W. Slope system reliability with general slip surfaces. Soils and Foundations 1994;34(3): 99–105. https://doi.org/10.3208/sandf1972.34.3_99.

37. Xiao T, Li D Q, Cao Z J, Tang X S. Full probabilistic design of slopes in spatially variable soils using simplified reliability analysis method. Georisk: Assessment and Management of Risk for Engineered Systems and Geohazards 2017;11(1):146-159. doi:10.1080/ 17499518. 2016. 1250279.

38. Ching J, Phoon K K, Hu Y G. Efficient evaluation of reliability for slopes with circular slip surfaces using importance sampling. Journal of Geotechnical and Geoenvironmental Engineering, American Society of Civil Engineers, 2009, 135(6):768–777. https://doi.org/ 10.1061/(ASCE)GT.1943-5606.0000035.

39. Low B K, Zhang J, Tang W H. Efficient system reliability analysis illustrated for a retaining wall and a soil slope. Computers and Geotechnics 2011;38(2): 196–204. https://doi.org/10.1016/j.compgeo.2010.11.005.

40. Cho S E. First-order reliability analysis of slope considering multiple failure modes. Engineering Geology 2013;154: 98–105. https://doi.org/10.1016/j.enggeo.2012.12.014.

41. Kang F, Xu Q, Li J. Slope reliability analysis using surrogate models via new support vector machines with swarm intelligence. Applied Mathematical Modelling 2016;40(11-12): 6105–6120. https://doi.org/10.1016/j.apm.2016.01.050.

42. Tang L S, Zhao Z L, Luo Z G, Sun Y L. What is the role of tensile cracks in cohesive slopes?. Journal of Rock Mechanics and Geotechnical Engineering 2019;11(2): 314–324. https://doi.org/10.1016/j.jrmge.2018.09.007.

43. ACADS. Soil slope stability programs review. Association for Computer Aided Design (Autralia). Melbourne. 1989.

44. Cheng Y M, Li L, Chi S C. Performance studies on six heuristic global optimization methods in the location of critical slip surface. Computers and Geotechnics 2007;34(6): 462–484. https://doi.org/10.1016/j.compgeo.2007.01.004.